doi:10.36487/ACG_repo/2435_R-10
9th International Conference and Exhibition on Mass Mining, Kiruna Sweden 17-19 September 2024

Establishing relations between seismic activity and production

D. J. Birch[a], A. Rigby[a], K. Simanjuntak[b], F. Mardiansyah[b] and E. Bayar[b]

[a]*Institute of Mine Seismology, Tasmania, Australia*

[b]*Rio Tinto Oyu Tolgoi, Ulaanbaatar, Mongolia*

ABSTRACT

Micro-seismic activity at a mine is typically strongly controlled by production activity. It is possible to quantify this relation between production and seismicity via a statistical model, which provides a potential means for managing the seismic response to future mining. This was demonstrated by establishing models relating simple parameters of production (tonnes fired and tonnes bogged) to parameters of the seismic response (event count and cumulative potency) at a block caving mine. Using these simple production parameters alone omits some important factors (such as rock mass condition, mining configuration, etc), and so the fit to the seismic response is naturally somewhat limited. We demonstrate that this fit can be improved by including an auto-regressive term into the model, which comes at the cost of limiting the model's forecasting horizon.

1 INTRODUCTION

The seismic response recorded at a mine is typically strongly influenced by production volumes and rates (Mendecki, 2013). Depending on the nature of this response it can potentially pose a hazard to miner safety and production, which motivates for the development of statistical models to forecast and thereby, mitigate the exposure to seismic hazard (Woodward et al., 2017, Martinsson and Tornman, 2020, de Beer, 2022). These models also have potential utility for short-term forecasting or even the management of future seismic response.

The nature of the models developed will depend on available data and the features of the seismic response that are of interest. Several approaches were previously published for different such contexts; for example, Martinsson and Tornman (2020) developed a hierarchical Bayesian model to describe the response (in terms of cumulative potency) to production (in terms of tonnes produced) across multiple sublevel caving operations at Malmberget mine in Sweden. Jakubowski (2014) utilised neural networks and stochastic gradient boosted trees to forecast monthly seismic energy release in response to longwall mining at the Bielszowice colliery in Poland. The monthly seismic response was parameterised in terms of several parameters including total face advance.

In this paper, a case study is presented using data from Oyu Tolgoi mine, a block caving mine in Mongolia operated by Rio Tinto. The seismic and production data used is outlined in Section 2. In Section 3, statistical models are developed relating seismicity in two seismogenic zones to production. The paper is concluded in section 4.

2 DATA

Data for the period 1 January 2022 to 31 December 2023 was selected, which includes the start of drawbell development in January 2022 and production bogging in June 2022. Figure 1 shows columns representing draw height, locations of drawbells and associated seismic response as of 31 December 2023.

The seismic response was divided into two distinct populations either side of the West Bat fault. Events above the footprint of the Panel Zero block cave (hereafter referred to as cave events) define a large cave yield zone, while those on the northwestern abutment (hereafter referred to as NW events and contained in the blue polygon in Figure 1) are characterised as often large, shear-type events. Stark contrasts in the seismic response are attributed to differences in the rock mass properties and in-situ stress orientation. A detailed description of the geology can be found in Porter (2016).

Figures 2 and 3 characterise the seismic response in each volume. Overall, there are far fewer NW events than cave events (by a factor of 20-30), but the significantly shallower size distribution (Figure 2) means that the cumulative potency is approximately double that of the cave events (Figure 3).

Based on the size distributions shown in Figure 2, events with moment magnitudes below -1.0 were excluded from the analysis to avoid any bias resulting from spatial variability in the sensitivity of the sensor array. This has left a set of 54,421 events for analysis, which were quantified in terms of two simple parameters:

- number of events per week and
- cumulative potency per week.

Our aim is to relate these response parameters to input parameters based on production and previous seismic response. In particular, the following three input parameters were considered:

- tonnes bogged per week,
- tonnes fired per week, and
- cumulative event count/potency in the previous week.

The response variables were plotted against each of the input variables in Figures 4 and 5, which are coloured according to region (Cave/NW). Based on the Spearman correlation coefficients listed in each plot, it can be seen that there are moderate to strong positive correlations across both regions between the seismic response (in terms of number of events or cumulative potency) and both the tonnes bogged and previous seismic response.

There are also moderate correlations between the response in each region and the tonnes fired. Interestingly, this correlation is negative in the case of the NW region. This is spurious (i.e., not causative) and most likely a result of each response being correlated with some other factor.

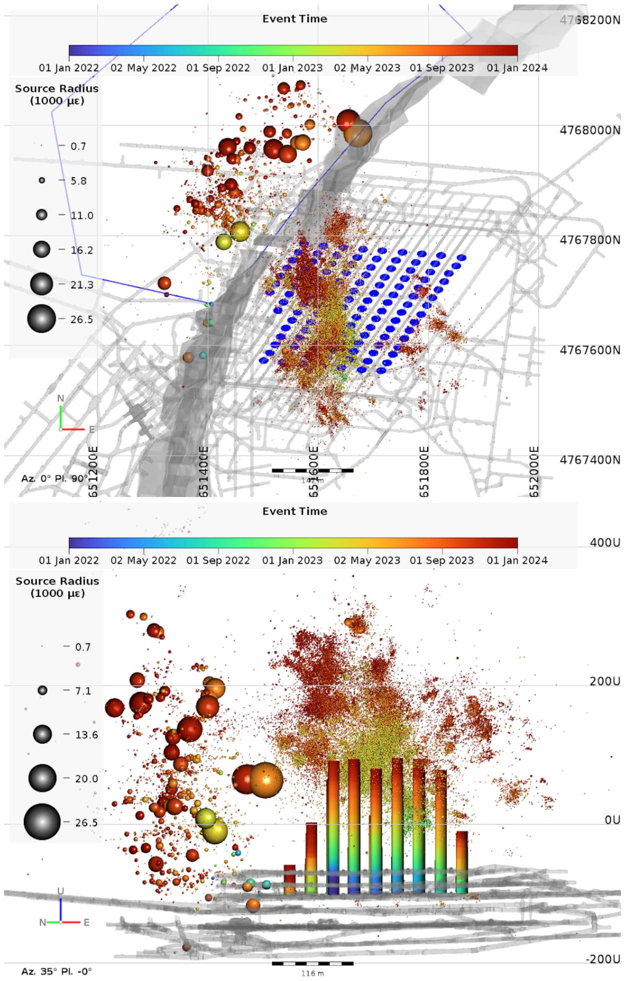

Figure 1 Distribution of the seismic response (mL ≥ -1.0), drawbells and draw heights at Panel Zero between 1 Jan 2022 and 31 Dec 2023. The events are sized by source radius assuming a constant strain change of 10-4 per unit potency.

Pairwise plots comparing the input parameters against one another are shown in Figure 6. Several (mostly unsurprising) correlations can be seen. The most prominent correlations are those between the number and cumulative potency of events recorded in the previous week. This correlation is especially strong for Cave events given the nature of the size distribution in that region (Figure 2).

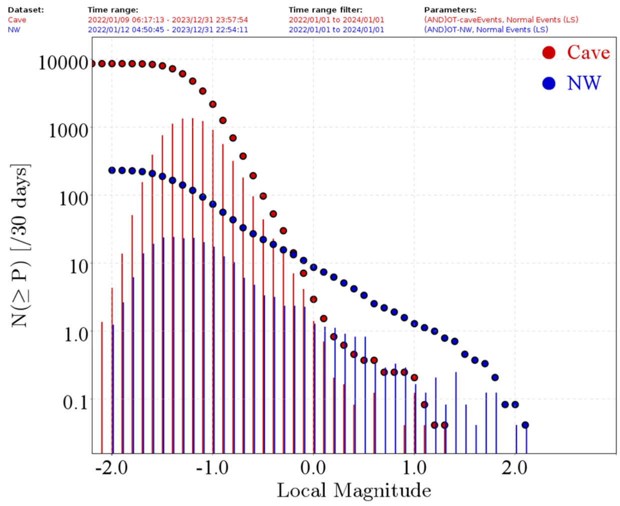

Figure 2 Size distribution plot showing two distinct populations.

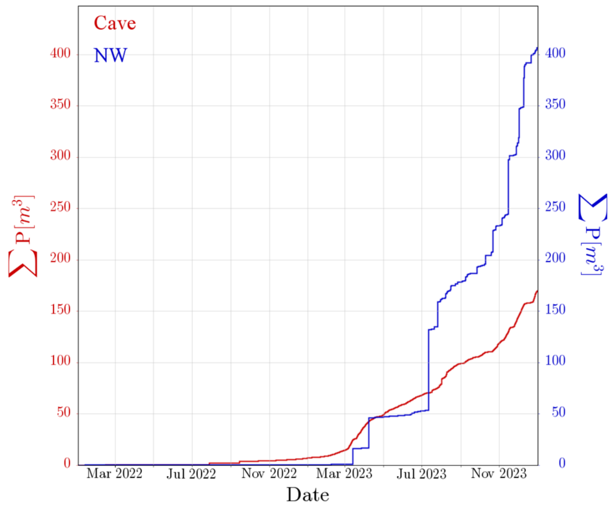

Figure 3 Cumulative seismic potency showing larger potency release per event on the NW abutment.

3 STATISTICAL MODELS

3.1 Number of events - Cave

A parametrisation of the seismic response in the Cave region in terms of tonnes blasted and bogged was first considered. In particular, a generalised linear model of the form,

$$\begin{aligned} E[N|T_{\mathrm{bog}}, T_{\mathrm{blast}}] = \exp(&\alpha_1 \\ &+ \alpha_{\mathrm{bog}} \log_{10} T_{\mathrm{bog}} \\ &+ \alpha_{\mathrm{blast}} \log_{10} T_{\mathrm{blast}}) \end{aligned} \tag{1}$$

was considered where N is number of events per week; T_{bog} is the tonnes bogged; T_{blast} is the tonnes blasted; and 1, α_{bog}, and blast are constants. To avoid complicating the analysis, weeks were omitted where there was no blasting or bogging. As the data is over-dispersed, the coefficients have been fitted using quasi-Poisson regression to yield,

$$\begin{aligned} E[N|T_{\mathrm{bog}}, T_{\mathrm{blast}}] &= \exp(-9.98 \\ &\quad + 3.80 \log_{10} T_{\mathrm{bog}} \\ &\quad - 0.158 \log_{10} T_{\mathrm{blast}}) \\ &= 4.65 \times 10^{-5} T_{\mathrm{bog}}^{1.65} T_{\mathrm{blast}}^{-0.0681} \end{aligned} \tag{2}$$

It can be seen that the coefficient for the blasting term is negative, which would suggest an increasing the total blasted volume results in a reduced seismic response, a somewhat counter-intuitive result. However, an F-test comparing the model of Eq. 2 to a null model with the blasting term removed reveals that it is not statistically significant ($F_{1,77}$ = 0.0466, p = 0.830).

Removing the blasting term and refitting a model of the form,

$$E[N|T_{\mathrm{bog}}] = \exp(\alpha_1 + \alpha_{\mathrm{bog}} \log_{10} T_{\mathrm{bog}}), \tag{3}$$

yields,

$$\begin{aligned} E[N|T_{\mathrm{bog}}] &= \exp(-10.5 \\ &\quad + 3.77 \log_{10} T_{\mathrm{bog}}) \\ &= 2.67 \times 10^{-5} T_{\mathrm{bog}}^{1.64} \end{aligned} \tag{4}$$

The remaining bogging term is significant ($F_{1,78}$ = 130, p < 0.001). The model provides a reasonable fit to the data, particularly in 2023 as shown in Figure 7. The poor fit to the observed seismic response during the early stages of production suggests that the model omits important variables (rock mass condition, mining configuration, etc.).

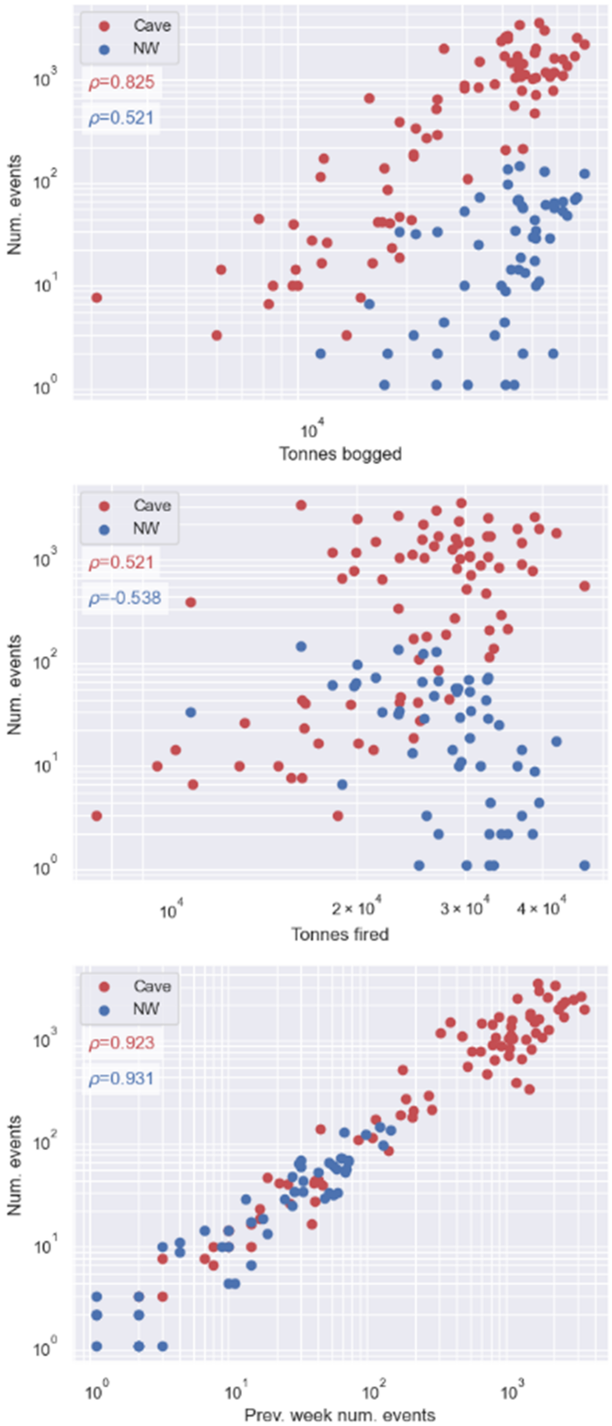

Figure 4 **Number of events recorded each week plotted against three basic input parameters. Spearman correlation coefficients are listed in the top left of each plot. Data for events associated with the cave are coloured red while those in the NW are blue.**

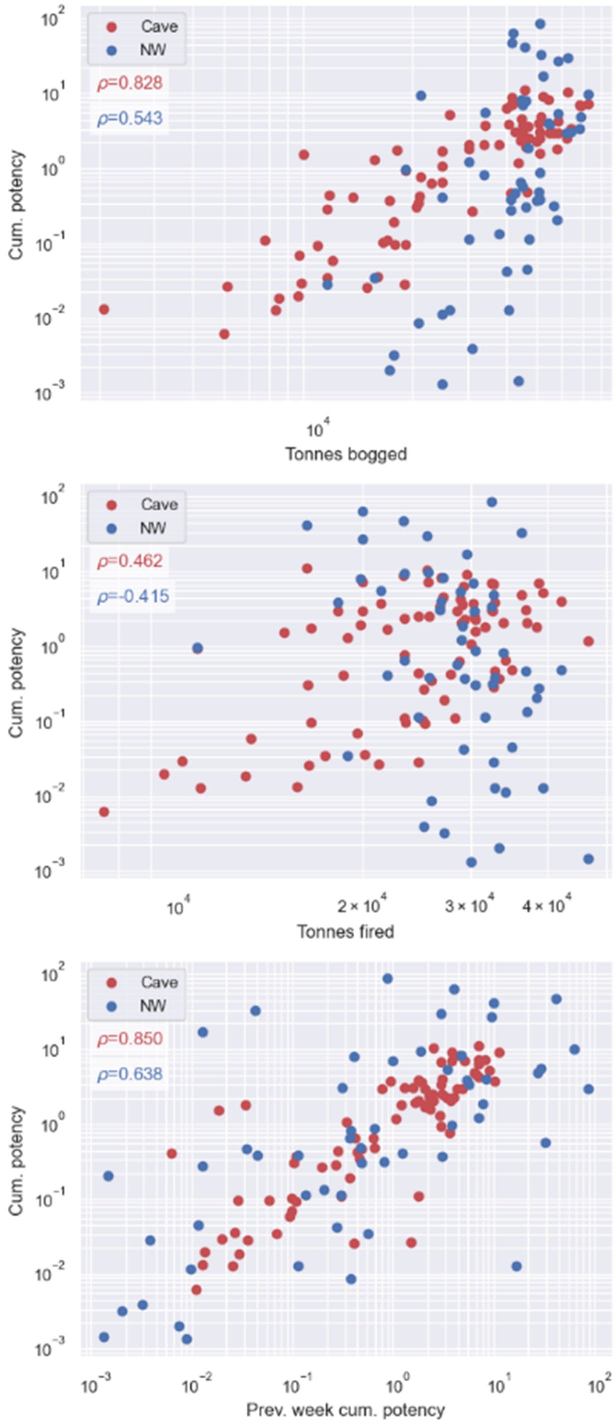

Figure 5 **Cumulative potency recorded each week plotted against three basic input parameters. Spearman correlation coefficients are listed in the top left of each plot. Data for events associated with the cave are coloured red while those in the NW are blue.**

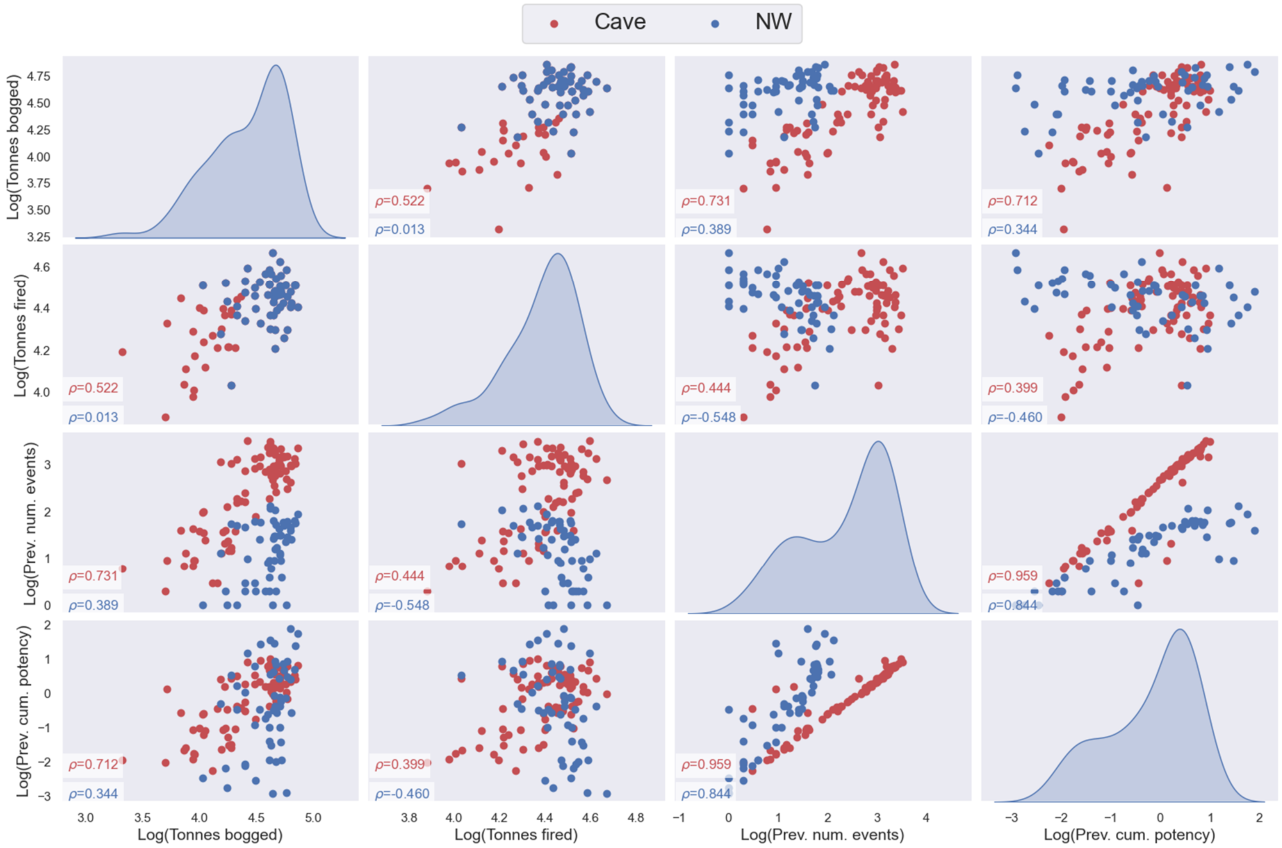

Figure 6 Log-transformed Pairwise relations between the basic parameters considered. Spearman correlation coefficients are listed in the lower left of each plot.

Assuming that the effect of these variables tends to vary on time scales on the order of a week or greater, we can expect to account for them (at least partially) by including an auto-regressive term in the model. In particular, a model of the form,

$$E[N|T_{\text{bog}}, N_{\text{prev}}] = \exp(\alpha_1 + \alpha_{\text{bog}} \log_{10} T_{\text{bog}} + \alpha_{\text{prev}} \log_{10} N_{\text{prev}}) \quad (5)$$

where N_{prev} is the number of events recorded in the previous week. Fitting this to the data yields,

$$\begin{aligned} E[N|T_{\text{bog}}, N_{\text{prev}}] &= \exp(-5.70 + 1.76 \log_{10} T_{\text{bog}} + 1.52 \log_{10} N_{\text{prev}}) \\ &= 3.35 \times 10^{-3} T_{\text{bog}}^{0.764} N_{\text{prev}}^{0.661} \end{aligned} \quad (6)$$

The terms for tonnes bogged and number of events in the previous week are both significant ($F_{1,77} = 36.5$, $p < 0.001$, and $F_{1,77} = 155$, $p < 0.001$, respectively). As can be seen in Figure 8, this model provides a much better fit to the observed data.

It is important to note that the inclusion of the auto-regressive term means this model should only be used for forecasting one week ahead. The inclusion of a term based on the cumulative potency recorded in the previous week was not considered given that, as discussed in Section 2, it is strongly correlated with event count and so adds little extra information.

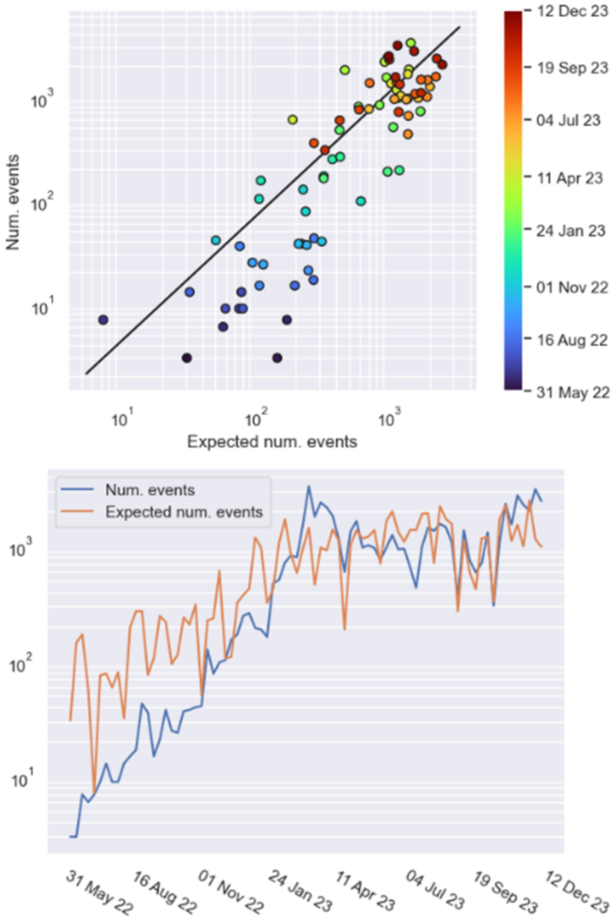

Figure 7 Comparison of observed number of cave events per week with expected calculated using Eq. 4.

3.2 Cumulative potency - Cave

A general linear model is considered for the parametrisation of cumulative potency in the Cave region, taking the form,

$$E[\log_{10}\Sigma P|T_{\text{bog}},T_{\text{blast}}] = \alpha_1 + \alpha_{\text{bog}}\log_{10}T_{\text{bog}} + \alpha_{\text{blast}}\log_{10}T_{\text{blast}} \quad (7)$$

Performing ordinary least squares regression to estimate the three constants yields,

$$E[\log_{10}\Sigma P|T_{\text{bog}},T_{\text{blast}}] = -11.5 + 2.08\log_{10}T_{\text{bog}} + 0.502\log_{10}T_{\text{blast}} \quad (8)$$

The terms for tonnes bogged is a significant improvement over the null model ($F_{1,77} = 121.0$, $p < 0.001$) whereas tonnes fired is not $F_{1,77} = 1.63$, $p = 0.255$). The tonnes fired term was therefore dropped giving the form,

$$E[\log_{10}\Sigma P|T_{\text{bog}}] = \alpha_1 + \alpha_{\text{bog}}\log_{10}T_{\text{bog}} \quad (9)$$

This yields,

$$E[\log_{10}\Sigma P|T_{\text{bog}}] = -10.0 + 2.23\log_{10}T_{\text{bog}} \quad (10)$$

The remaining term is significant ($F_{1,78} = 221$, $p < 0.001$) and the model provides a reasonable fit to the observed data (Figure 9).

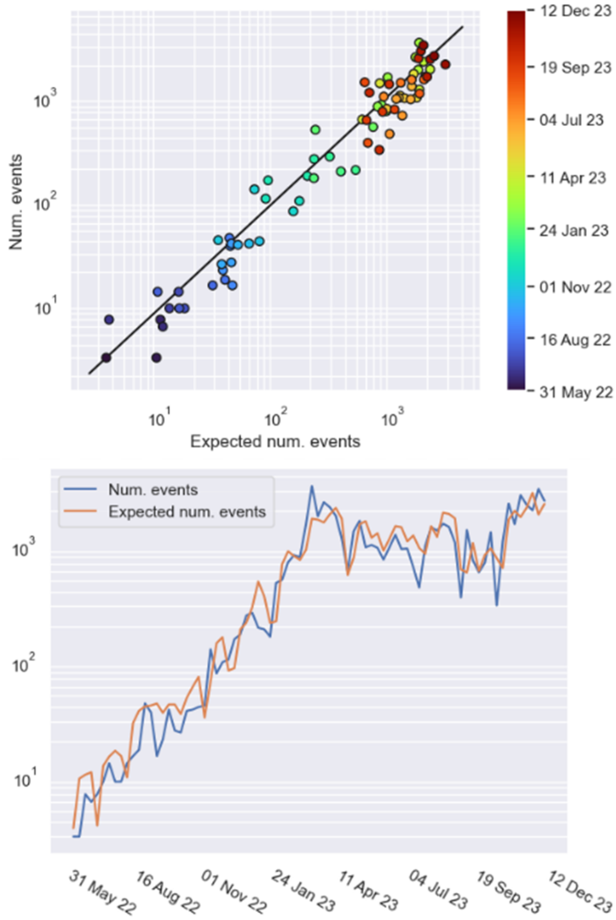

Figure 8 Comparison of observed number of cave events per week with expected calculated using Eq. 6.

The fit was further improved by the inclusion of the auto-regressive term, observed cumulative potency in the previous week.

$$E[\log_{10}\Sigma P|T_{\text{bog}},\Sigma P_{\text{prev}}] = \alpha_1 + \alpha_{\text{bog}}\log_{10}T_{\text{bog}} + \alpha_{\text{prev}}\log_{10}\Sigma P_{\text{prev}} \quad (11)$$

Fitting the data to this form yields,

$$E[\log_{10} \Sigma P | T_{\text{bog}}, \Sigma P_{\text{prev}}] = -6.49 + 1.45 \log_{10} T_{\text{bog}} + 0.386 \log_{10} \Sigma P_{\text{prev}} \quad (12)$$

Both terms were a significant improvement over the null model with $F_{1,77} = 51.2$, $p < 0.001$ and $F_{1,78} = 25.2$, $p < 0.001$, respectively. The performance of Eq. 12 in Figure 10 is only marginally better than that of Eq. 10 shown in Figure 9.

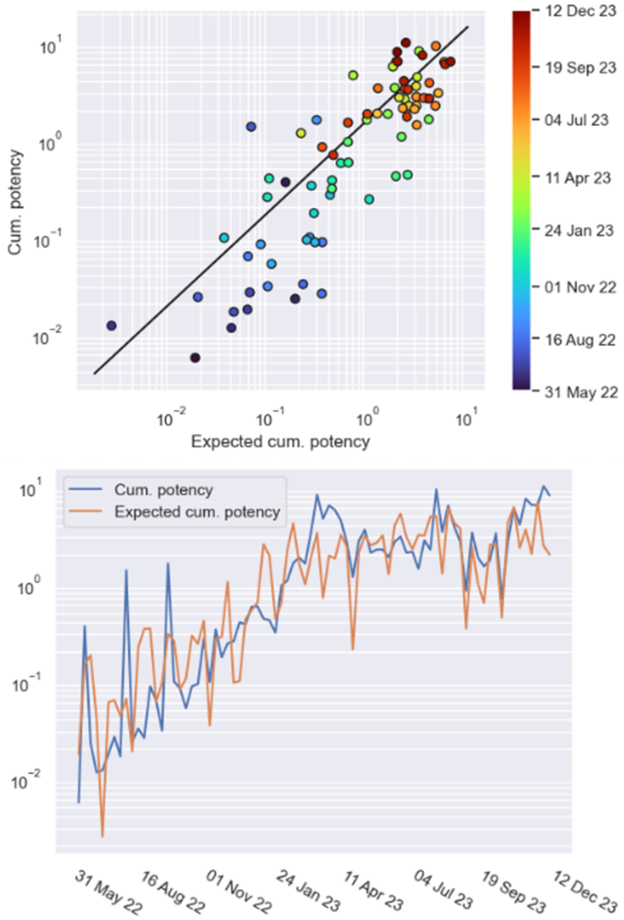

Figure 9 Comparison of the observed cumulative potency per week in the cave region and expected as calculated using Eq. 10.

The three large jumps in cumulative potency between May and Nov 2022 are attributed to the occurrence of the four largest events in this dataset. The hypocentre locations are on the NW abutment, very close to the West Bat fault (Figure 1) but do not form part of the cluster of seismic activity in the NW. The inclusion of these four events as "Cave" events may be debatable, but it does not significantly influence the results of this study.

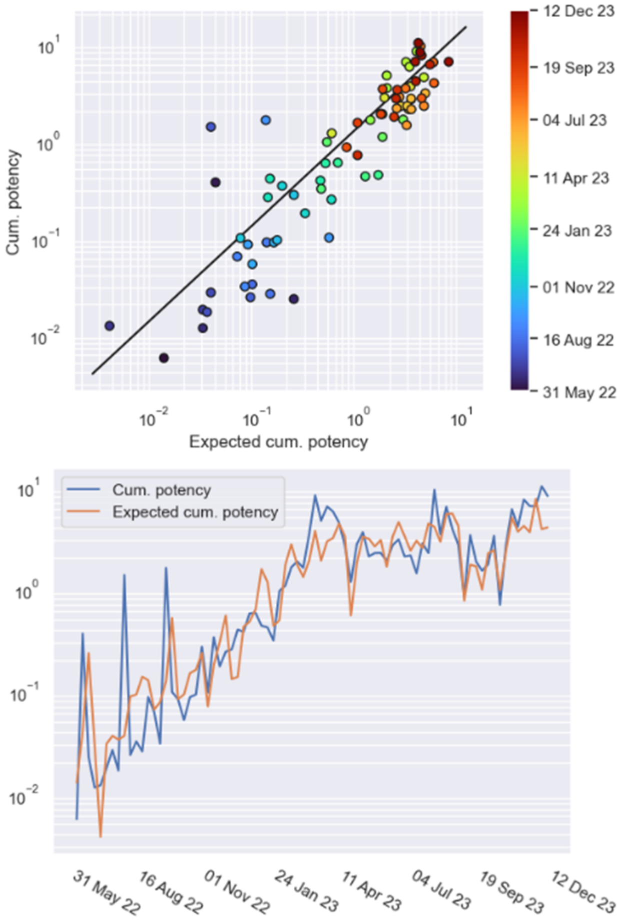

Figure 10 Comparison of the observed cumulative potency per week in the cave region and expected as calculated using Eq. 12.

3.3 *Number of events - NW*

The approach was repeated in Section 3.1 with a parameterisation of the number of events per week recorded in the seismically active volume NW of Panel Zero (Figure 1). A model of the form given in Eq. 3 was considered and fitted using quasi-Poisson regression to yield,

$$E[N | T_{\text{bog}}] = \exp(-11.8 + 3.29 \log_{10} T_{\text{bog}}) = 7.74 \times 10^{-6} T_{\text{bog}}^{1.43} \quad (13)$$

The tonnes bogged term is significant ($F1{,}52 = 16.3$, $p < 0.001$). As seen in Figure 7 (Section 3.1), the earliest data is more scattered while a reasonably good match is observed for most of 2023. Note a term for tonnes blasted was not considered given that we expect its correlation with the seismic response in the NW region to be spurious (see Section 2).

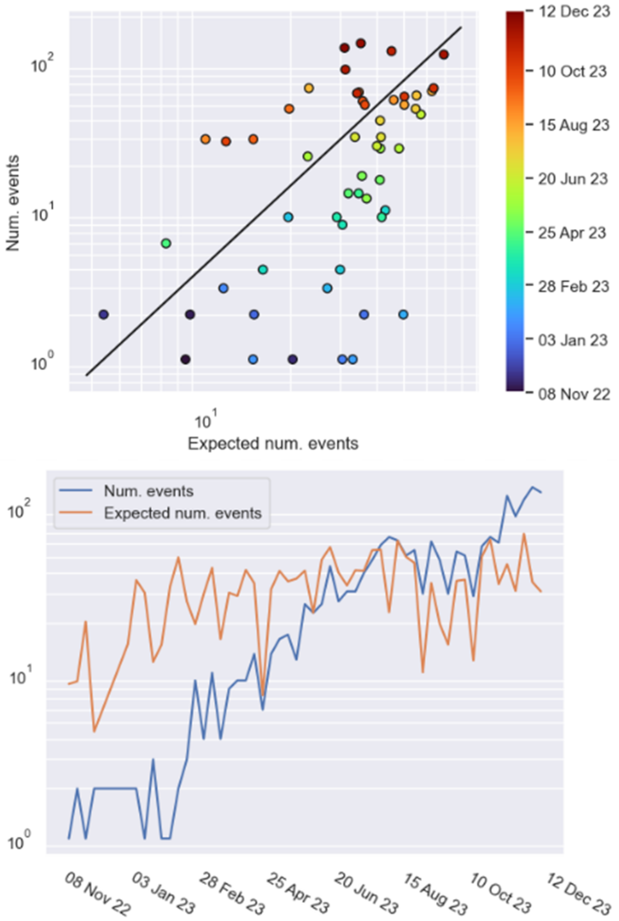

Figure 11 Comparison of observed number of NW events per week with expected calculated using Eq. 13.

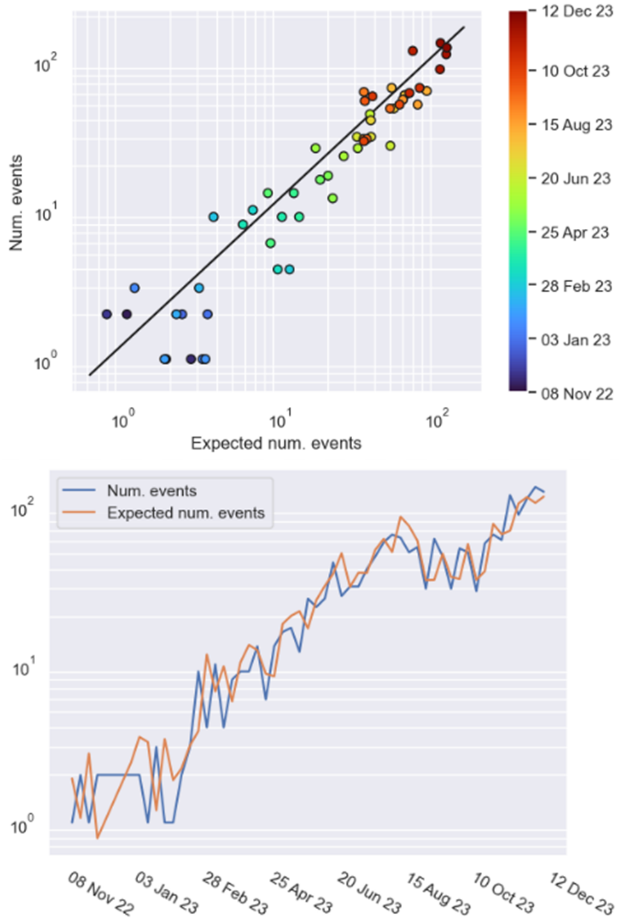

Figure 12 Comparison of observed number of NW events per week with expected calculated using Eq. 15.

Introducing the auto-regressive term gives the form,

$$E[N|T_{\text{bog}}, N_{\text{prev}}] = \exp(\alpha_1 + \alpha_{\text{bog}} \log_{10} T_{\text{bog}} + \alpha_{\text{prev}} \log_{10} N_{\text{prev}}) \quad (14)$$

Fitting Eq. 14 to the data yields,

$$\begin{aligned} E[N|T_{\text{bog}}, N_{\text{prev}}] &= \exp(-5.79 + 1.38 \log_{10} T_{\text{bog}} + 1.96 \log_{10} N_{\text{prev}}) \\ &= 3.05 \times 10^{-3} T_{\text{bog}}^{0.600} N_{\text{prev}}^{0.85} \end{aligned} \quad (15)$$

Tonnes bogged and number of events in the previous week are both statistically significant ($F1,51 = 21.7$, $p < 0.001$ and $F1,51 = 380$, $p < 0.001$, respectively). The resulting fit to the observed data is drastically improved but as stated earlier, this adjustment limits the appropriate forecasting horizon to one week.

3.4 Cumulative potency - NW

The process followed in Section 3.2 was repeated for data recorded in the NW cluster. Using ordinary least squares regression to fit the model represented by Eq. 9 yields,

$$E[\log_{10} \Sigma P|T_{\text{bog}}] = -18.5 + 3.97 \log_{10} T_{\text{bog}} \quad (16)$$

As with Section 3.3, tonnes bogged is statistically significant ($F_{1,52} = 24.4$ and $p < 0.001$).

The inclusion of an auto-regressive term leads to the form,

$$E[\log_{10} \Sigma P|T_{\text{bog}}, \Sigma P_{\text{prev}}] = \alpha_1 + \alpha_{\text{bog}} \log_{10} T_{\text{bog}} + \alpha_{\text{prev}} \log_{10} \Sigma P_{\text{prev}} \quad (17)$$

and yields,

$$E[\log_{10}\Sigma P|T_{\mathrm{bog}},\Sigma P_{\mathrm{prev}}] = -12.6 + 2.72\log_{10}T_{\mathrm{bog}} + 0.493\log_{10}\Sigma P_{\mathrm{prev}} \quad (18)$$

Tonnes bogged and cumulative potency in the previous week are significant ($F_{1,51} = 14.2$, $p < 0.001$ and $F_{1,51} = 23.4$, $p < 0.001$, respectively).

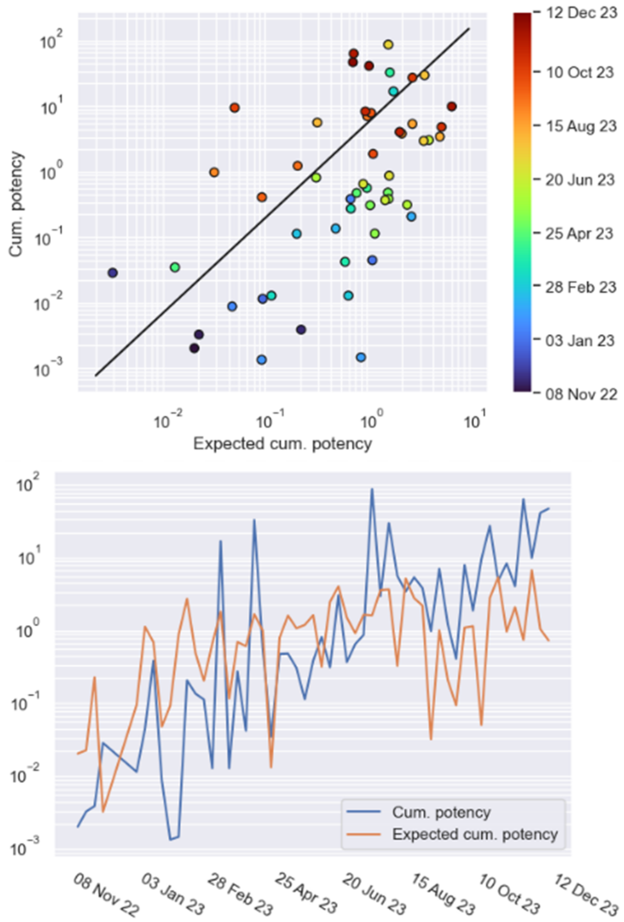

Figure 13 Comparison of observed number of NW events per week with expected calculated using Eq. 16.

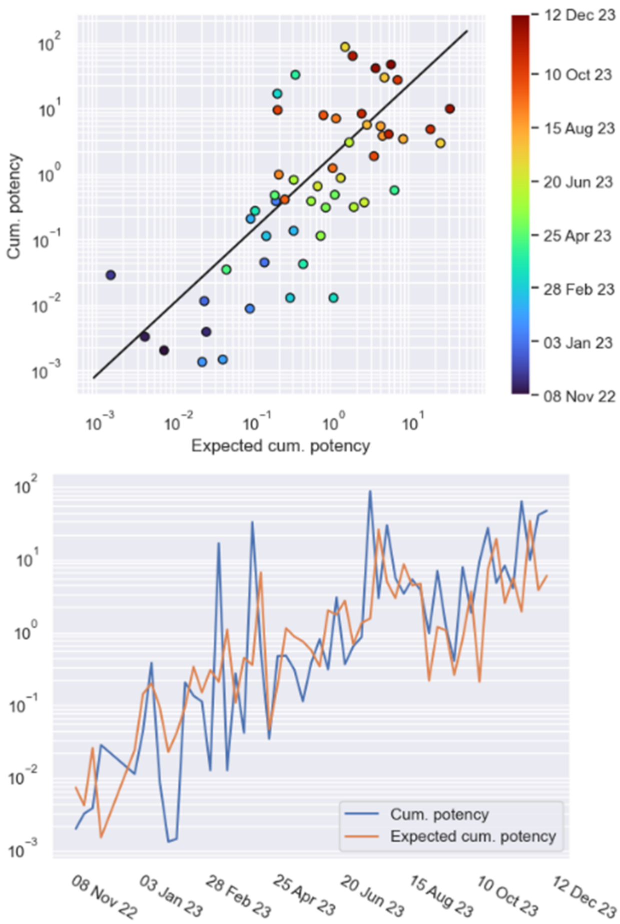

Figure 14 Comparison of the observed cumulative potency per week in the NW region with expected calculated using Eq. 18.

4 CONCLUSIONS

The recorded seismic response at Oyu Tolgoi mine between Jan 2022 and Dec 2023 was divided into two regions: Cave and NW. Statistical models were developed that relate the seismic response in each region in terms of event count and cumulative potency, to production in weekly intervals.

It was found that weekly tonnes bogged has a strong influence on seismicity in both regions. Conversely, blasting seems to have little influence on events in the cave region and a spurious negative correlation with the response in the NW region. The negative correlation is explained by the mining sequence. During cave initiation larger amounts were blasted weekly to progress the undercut ahead of drawbell development. Later on, as sustained caving was reached, the seismic response accelerated while tonnes blasted subsided.

The simple parameters considered in this paper (weekly tonnes blasted and tonnes bogged) omit important variables that can be expected to influence the seismic response (e.g., rock mass properties, mining configuration, etc.). It was shown that the inclusion of auto-regressive terms in the models based on the seismic response in the previous week can at least partially account for this missing information but it should be noted that this comes at the cost of limiting the forecasting horizon of the models.

The models presented in this paper are quite simple, and could be further developed in a number of ways. One possibility would be to use input variables that are the result of numerical stress modelling (e.g., loading system stiffness (Wiles, 2002) at the points of blasting and/or bogging), which may serve as an alternative to the auto-regressive terms without limiting forecasting power. A further consideration is to include spatial binning to investigate correlations between the seismic response and production for certain domains.

ACKNOWLEDGEMENT

The authors would like to thank Rio Tinto Oyu Tolgoi mine for providing high-quality data sets for use in this analysis.

REFERENCES

de Beer, W. (2022). Quantitative correlation of production and seismic response in block caves. In Y. Potvin (Ed.), Caving 2022: Proceedings of the Fifth International Conference on Block and Sublevel Caving, Australian Centre for Geomechanics, Perth, pp. 473-486, https://doi.org/10.36487/ACG_repo/2205_32.

Jakubowski, J. & Tajduś, A. (2014). Predictive regression models of monthly seismic energy emissions induced by longwall mining. *Arch. Min. Sci.*, Vol. 59, No 3, p. 705–720, https://doi.org/10.2478/amsc-2014-0049.

Martinsson, J. & Törnman, W. (2020). Modelling the dynamic relationship between mining induced seismic activity and production rates, depth and size: A mine-wide hierarchical model. Pure *Appl. Geophys*, 177 (2020), 2619–2639. https://doi.org/10.1007/s00024-019-02378-y.

Mendecki, A. J. (2013). Characteristics of seismic hazard in mines: Keynote lecture. 8th International Symposium on Rockbursts and Seismicity in Mines, September 2013, Petersburg-Moscow, Russia.

Porter, T. M. (2016). The geology, structure and mineralisation of the Oyu Tolgoi porphyry copper-gold-molybdenum deposits, Mongolia: A review. *Geoscience Frontiers*, Vol. 7, Issue 3 (pp. 375-407), https://doi.org/10.1016/j.gsf.2015.08.003.

Wiles, T. D. (2002). Loading system stiffness - a parameter to evaluate rockburst potential. In First International Seminar on Deep and High Stress Mining, Australian Centre for Geomechanics, Perth, Australia, 2002.

Woodward, K., Wesseloo, J. & Potvin, Y. 2017. 'The spatial and temporal assessment of clustered and time-dependent seismic responses to mining, in J Wesseloo (ed.), Deep Mining 2017: Proceedings of the Eighth International Conference on Deep and High Stress Mining, Australian Centre for Geomechanics, Perth, pp. 157-171, https://doi.org/10.36487/ACG_rep/1704_09_Woodward.